Supporting information for

Ordering-Driven Biaxial Strain Engineering in PtNi Intermetallic Nanowires for Oxygen Reduction Catalysis

Xing Hu[1,4], Shize Geng[2,4], Yu Cao[3,4], Kezhu Jiang[1,], Yibo Liu[1], Ruifan Li[1], Yangyang Zhang[1], Shuang Meng[1], Shan Zhu[1], Lingzheng Bu[2,*], Cong Chen[1,*] and Shijian Zheng[1,*]*

[1]Tianjin Key Laboratory of Materials Laminating Fabrication and Interface Control Technology, School of Materials Science and Engineering, Hebei University of Technology, Tianjin, 300401, China.

[2]College of Energy, Xiamen University, Xiamen, 361102, China.

[3]School of Mechanical and Resource Engineering, WuZhou University, Wuzhou, 543002, China

[4]These authors contributed equally: Xing Hu, Shize Geng, Yu Cao

[*]E-mail: kzjiang@hebut.edu.cn, lzbu@xmu.edu.cn, chencong@hebut.edu.cn, sjzheng@hebut.edu.cn

This supplementary file includes:

Supplementary Figures. S1 to 29

Supplementary Tables S1 to 3

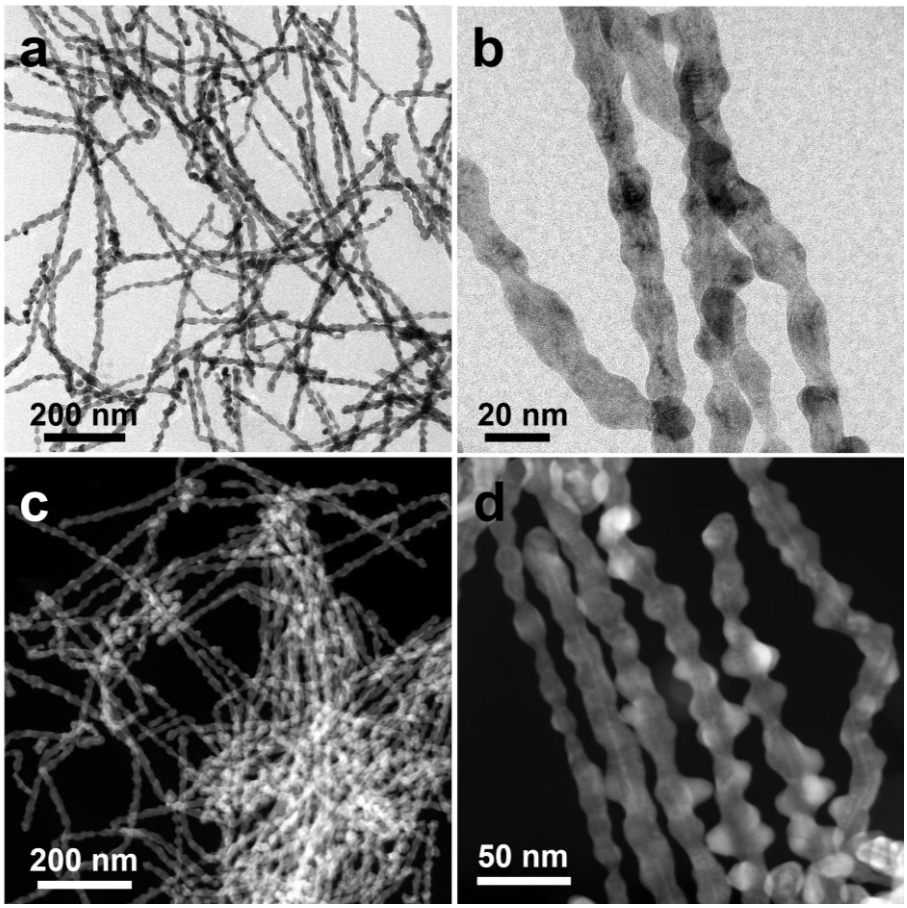

Figure S1. (a, b) TEM images and (c, d) STEM images of I-PtNi NWs.

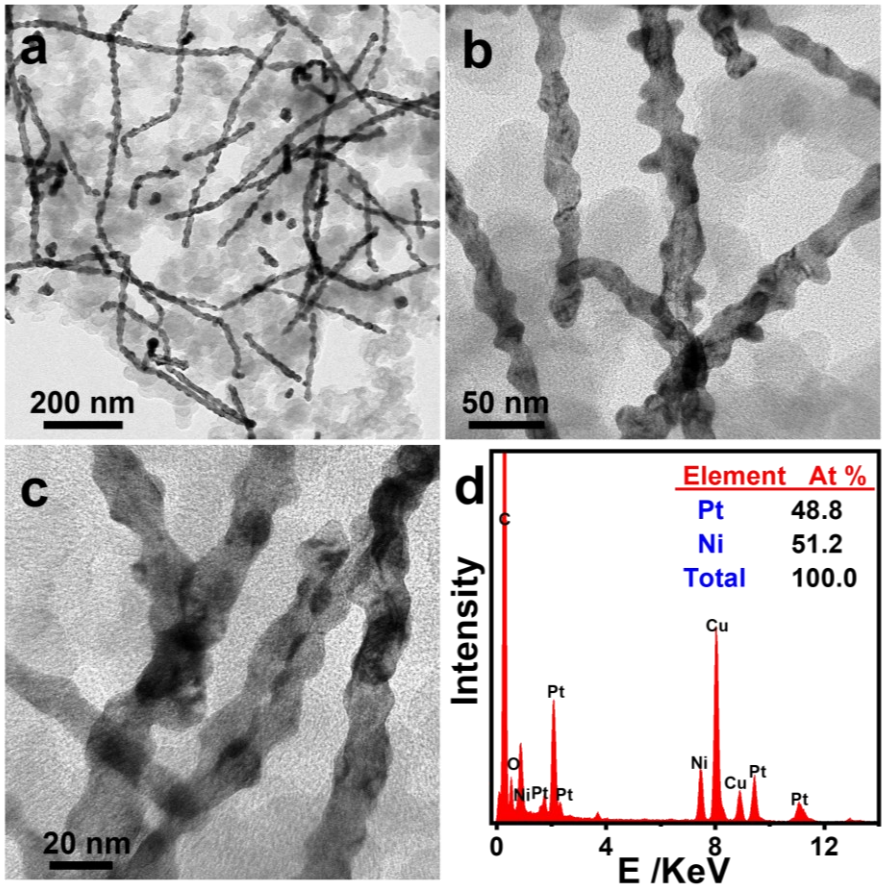

Figure S2. (a-c) TEM images and (d) EDS pattern of I-PtNi NWs/C.

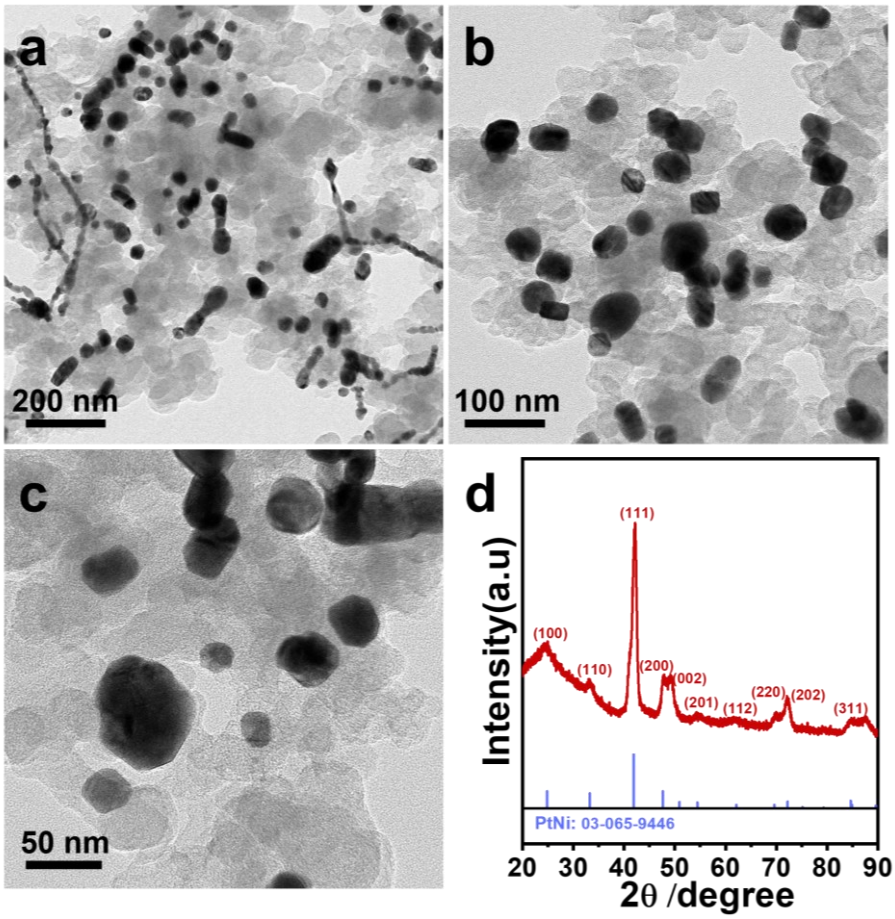

Figure S3. (a-c) TEM images and (d) XRD pattern of I-PtNi NWs/C annealed under Ar at 550°C for 5 h.

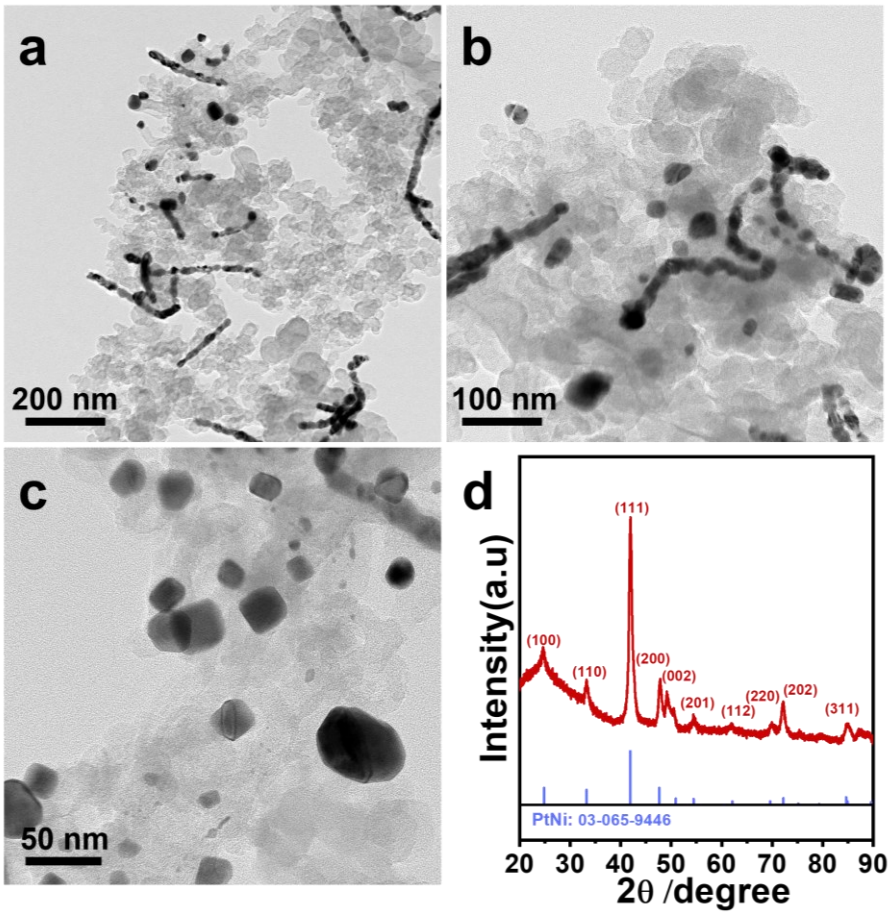

Figure S4. (a-c) TEM images and (d) XRD pattern of I-PtNi NWs/C annealed under vacuum (-0.1 MPa) at 550°C for 5 h.

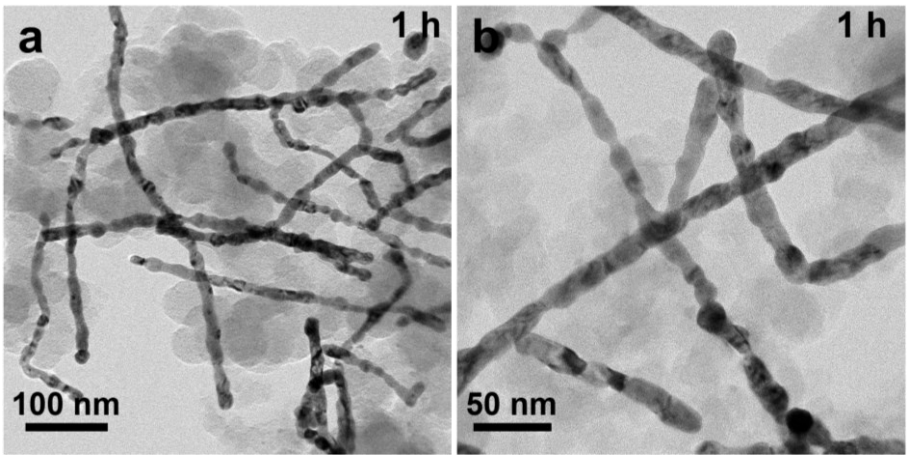

Figure S5. TEM images of I-PtNi NWs/C annealed at 550°C for 1 h.

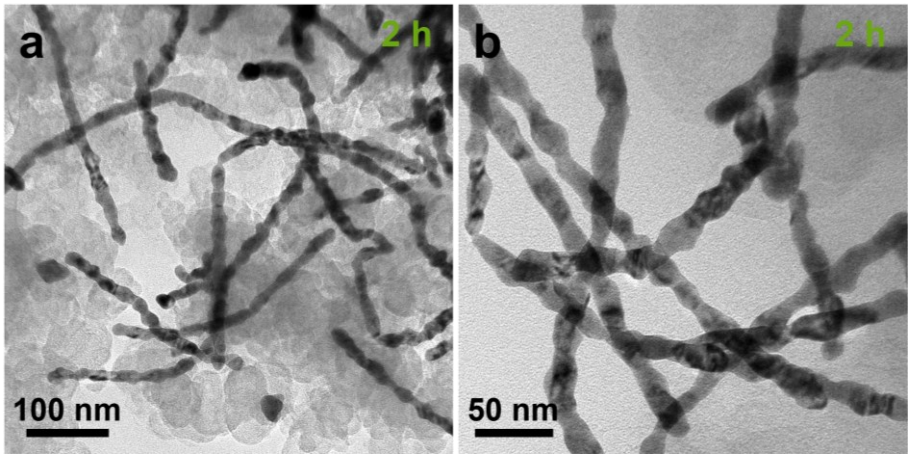

Figure S6. TEM images of I-PtNi NWs/C annealed at 550°C for 2 h.

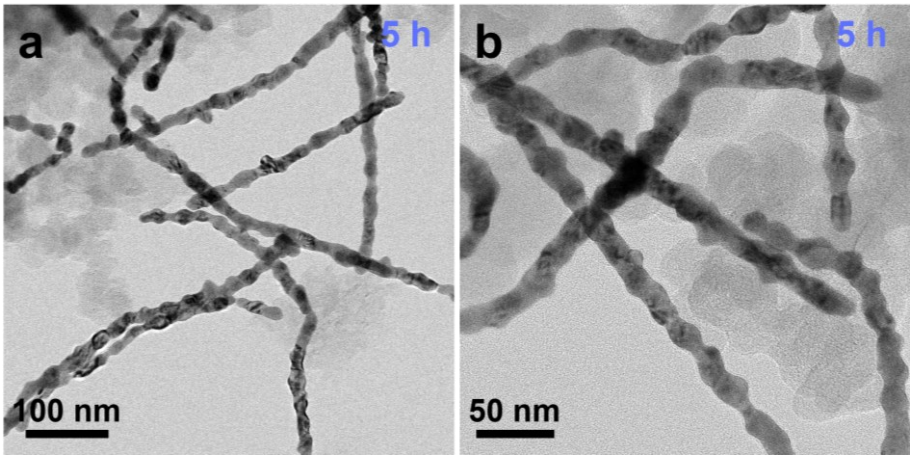

Figure S7. TEM images of I-PtNi NWs/C annealed at 550°C for 5 h.

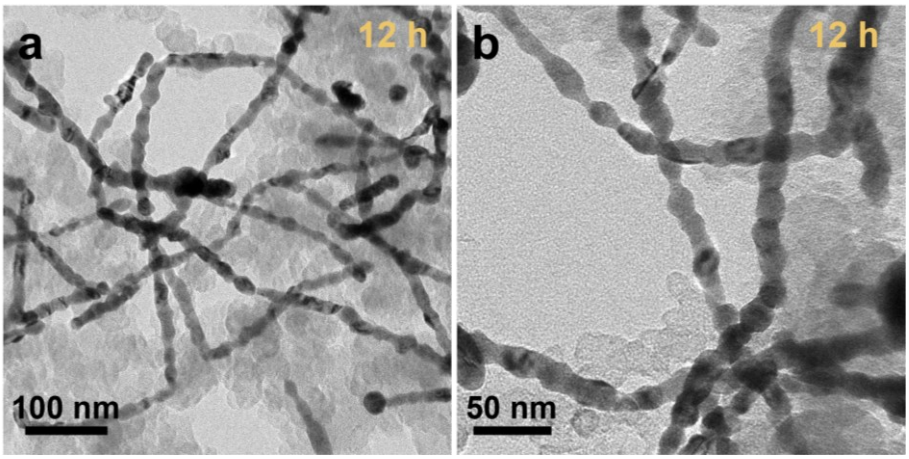

Figure S8. TEM images of I-PtNi NWs/C annealed at 550°C for 12 h.

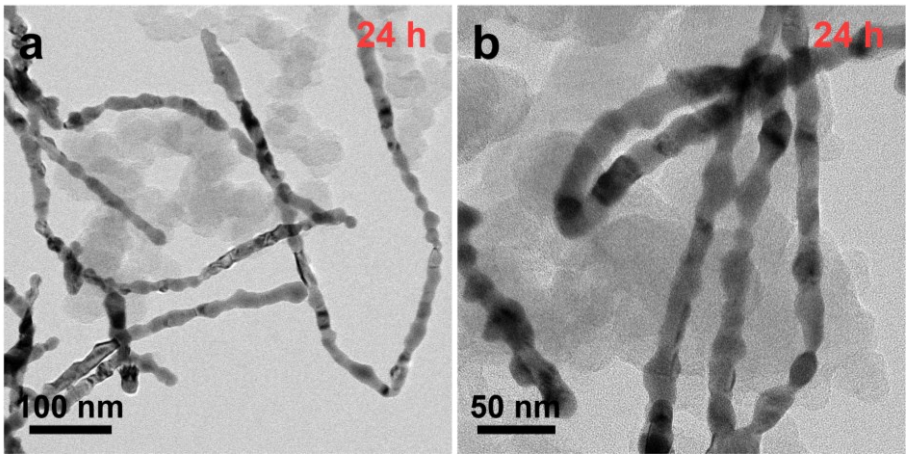

Figure S9. TEM images of I-PtNi NWs/C annealed at 550°C for 24 h.

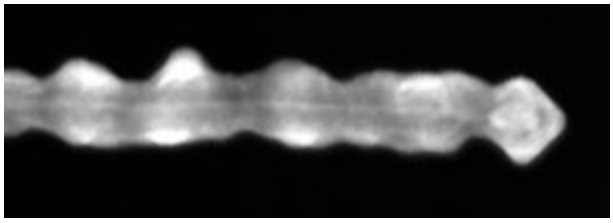

Figure S10. STEM image of I-PtNi NWs/C.

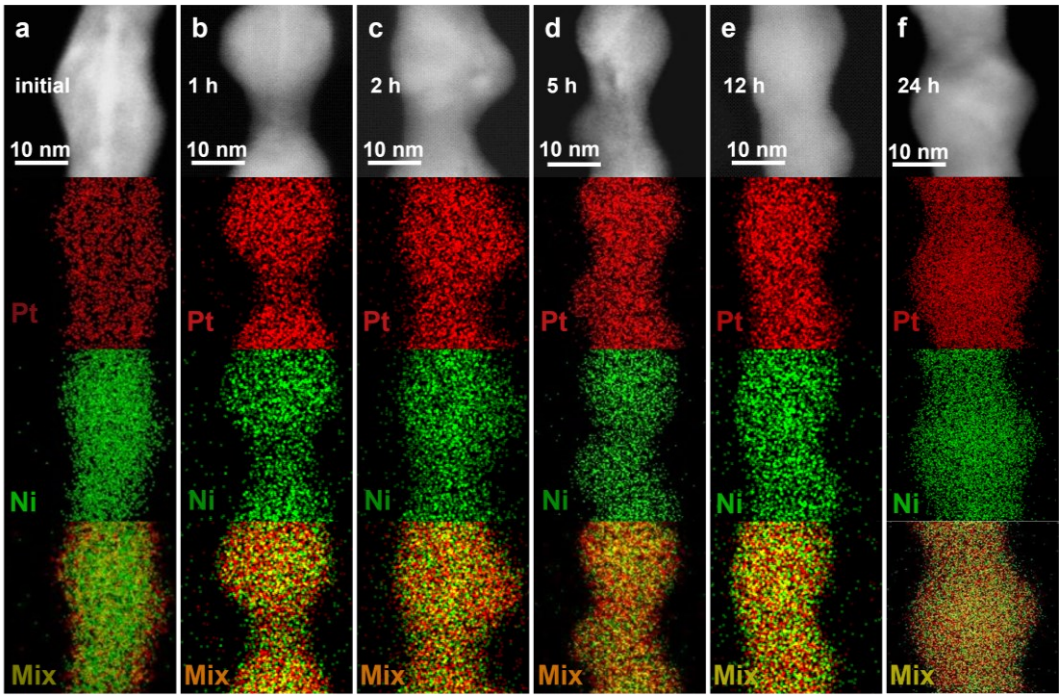

Figure S11. STEM images and STEM-EDS elemental mappings of I-PtNi NWs/C annealed at 550°C for (a) 0 h; (b) 1 h; (c) 2 h; (d) 5 h; (e) 12 h and (f) 24 h.

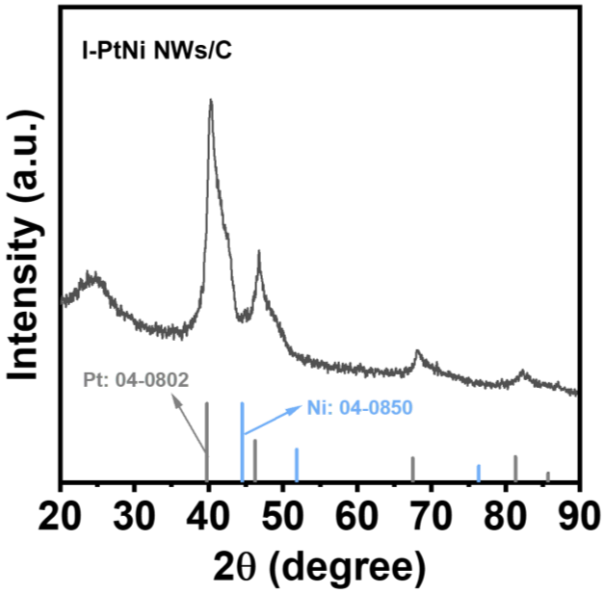

Figure S12. XRD pattern of I-PtNi NWs/C.

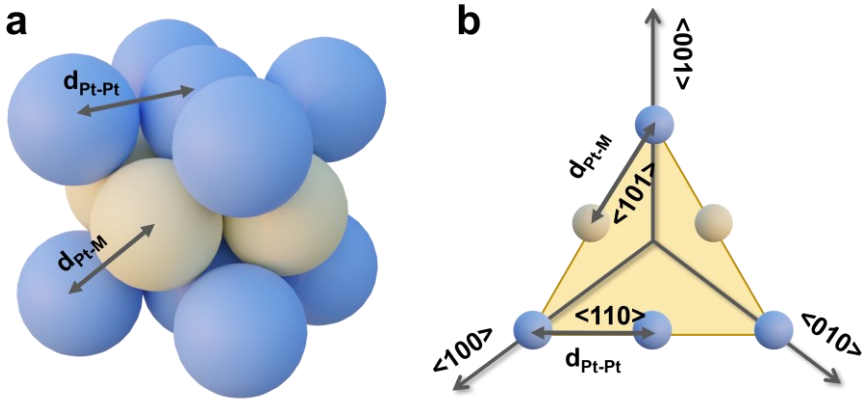

Figure S13. (a) Crystal structure of $L1_0$-PtNi. The lattice constant is a = b = 3.823 Å, c = 3.589 Å. (b) Schematic illustration of lattice mismatch on (111) facet. Blue and yellow spheres represent Pt and Ni atoms, respectively. Yellow plane represents (111) facet.

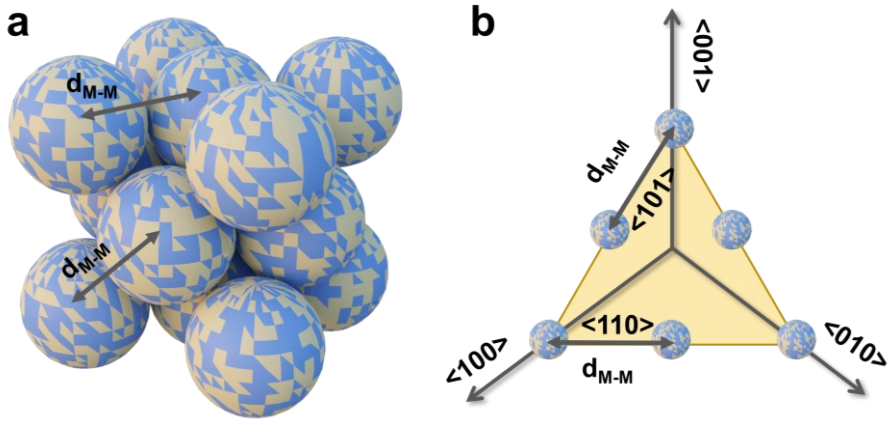

Figure S14. (a) Crystal structure of fcc-PtNi (M = Pt or Ni). The lattice constant is a = b = c = 3.750 Å. (b) Schematic illustration of lattice mismatch on (111) facet. Spheres represent Pt or Ni atoms, respectively. Yellow plane represents (111) facet.

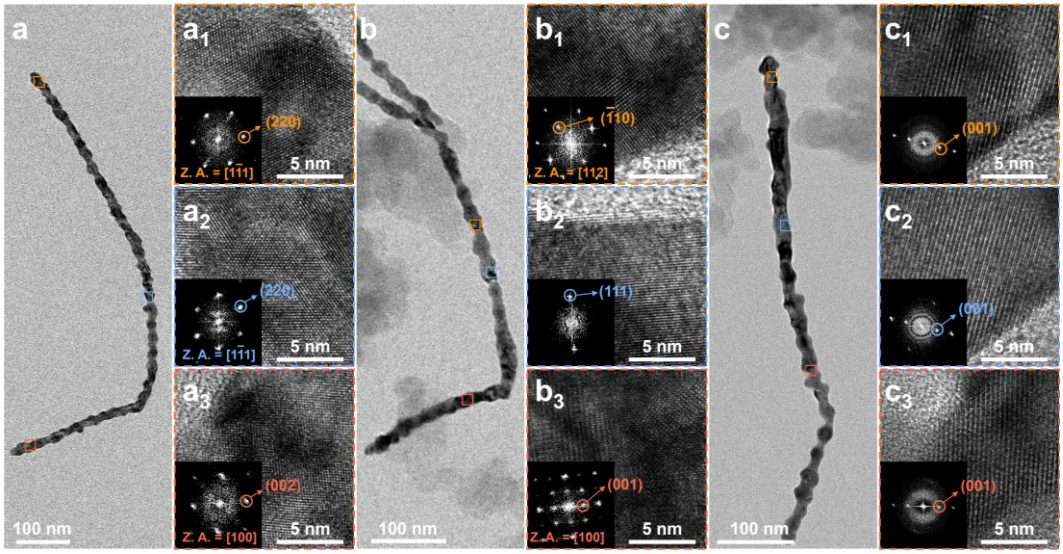

Figure S15. (a) TEM image of a representative D-PtNi NWs/C nanowire, along with HRTEM and corresponding FFT images of the regions highlighted in yellow, blue and orange. (b) TEM image of a representative M-PtNi NWs/C nanowire, with HRTEM and corresponding FFT images of the regions highlighted in yellow, blue and orange. (c) TEM image of a representative H-PtNi NWs/C nanowire, and the HRTEM and FFT images of of the regions highlighted in yellow, blue and orange.

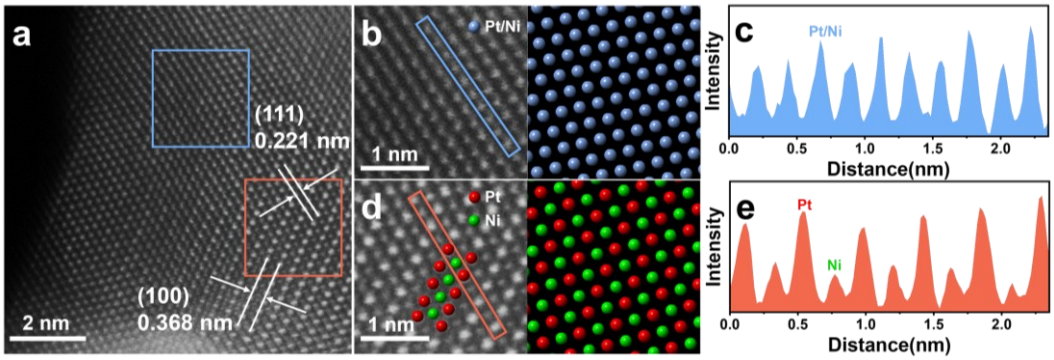

Figure S16. (a) High-magnification AC-HAADF-STEM image. (b) Enlarged view of the blue-marked region in (a) with the corresponding atomic configuration of fcc-PtNi. (c) Z-contrast intensity profile extracted from the region in (b). (d) Enlarged view of the orange-marked region in (a) with the corresponding atomic configuration of $L1_0$-PtNi along the [110] zone axis (e) Z-contrast intensity profile extracted from the region in (d).

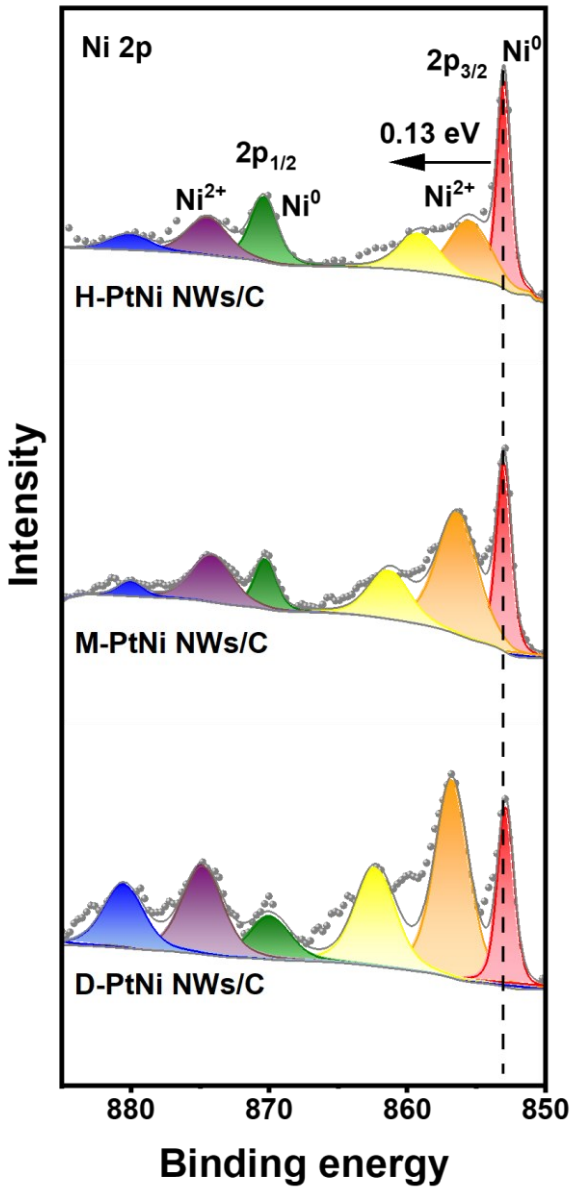

Figure S17. The XPS spectra of Ni 2*p* in (a) D-PtNi NWs/C, (b) M-PtNi NWs/C and (c) H-PtNi NWs/C.

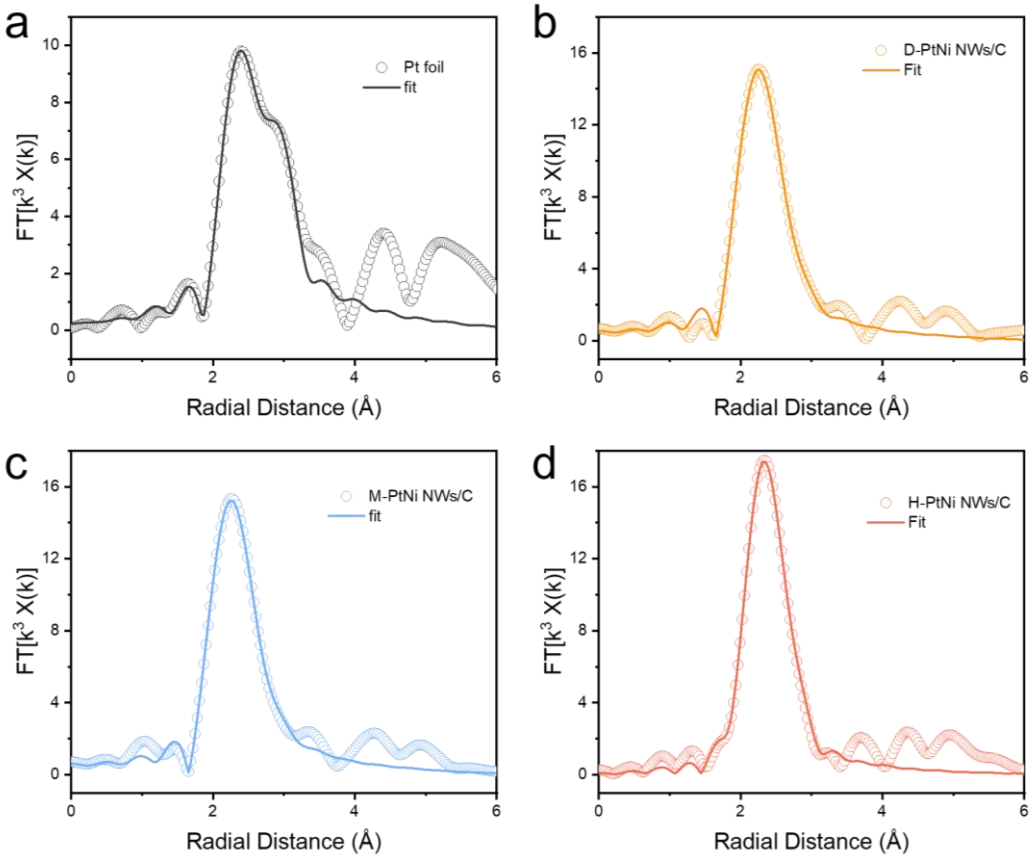

Figure S18. R space and inverse FT-EXAFS fitting results of Pt L_3-edge for (a) Pt foil (FT range: 3.0-10.0 Å^{-1}; fitting range: 1.0-3.0 Å), (b) D-PtNi NWs/C (FT range: 3.0-10.0 Å^{-1}; fitting range: 1.0-3.0 Å), (c) M-PtNi NWs/C (FT range: 3.0-10.0 Å^{-1}; fitting range: 1.0-3.0 Å), (d) H-PtNi NWs/C (FT range: 3.0-10.0 Å^{-1}; fitting range: 1.0-3.0 Å).

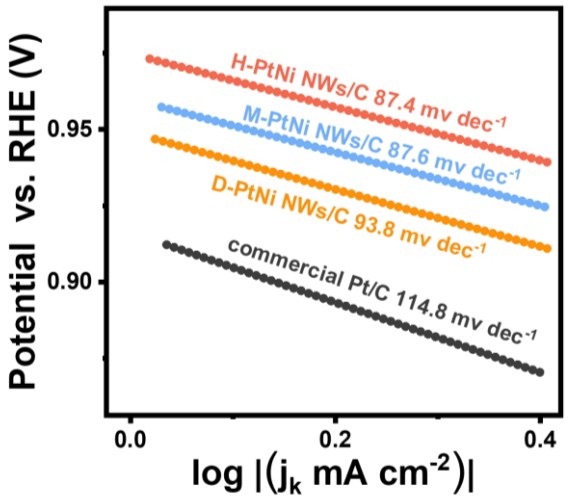

Figure S19. Tafel plots of D-PtNi NWs/C, M-PtNi NWs/C, H-PtNi NWs/C and commercial Pt/C.

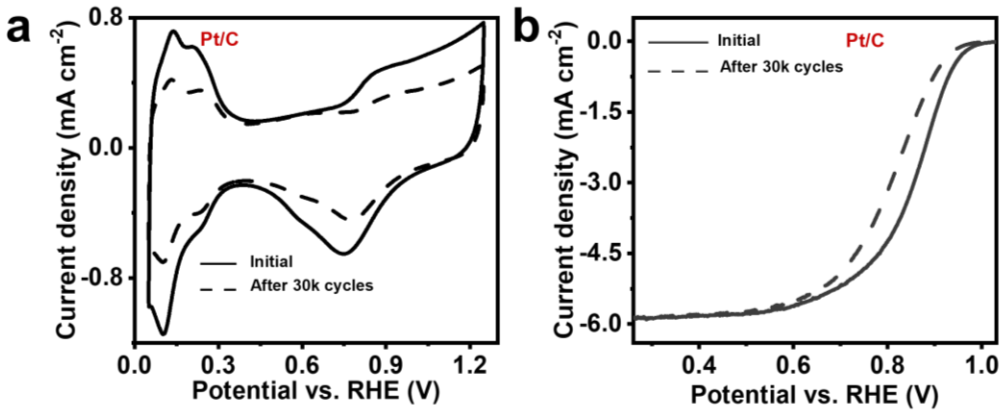

Figure S20. (a) CVs, (b) ORR polarization curves of commercial Pt/C before and after 30,000 potential cycles.

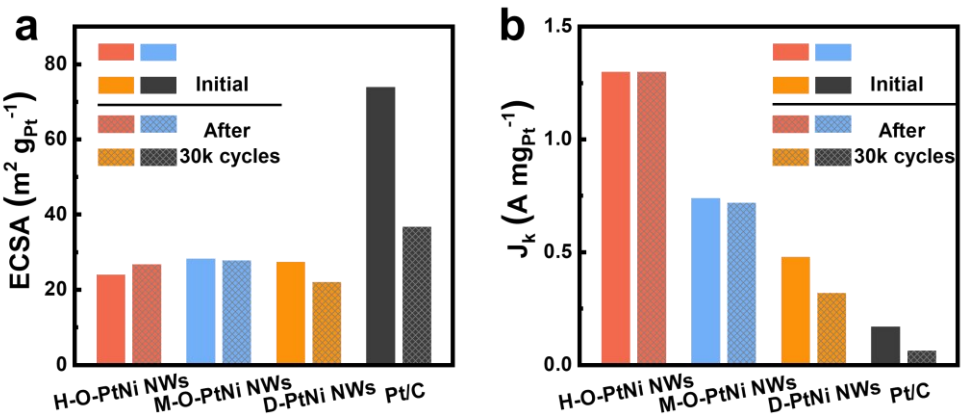

Figure S21. The changes in (a) ECSA, (b) mass activities of D-PtNi NWs/C, M-PtNi NWs/C, H-PtNi NWs/C and commercial Pt/C before and after 30,000 potential cycles.

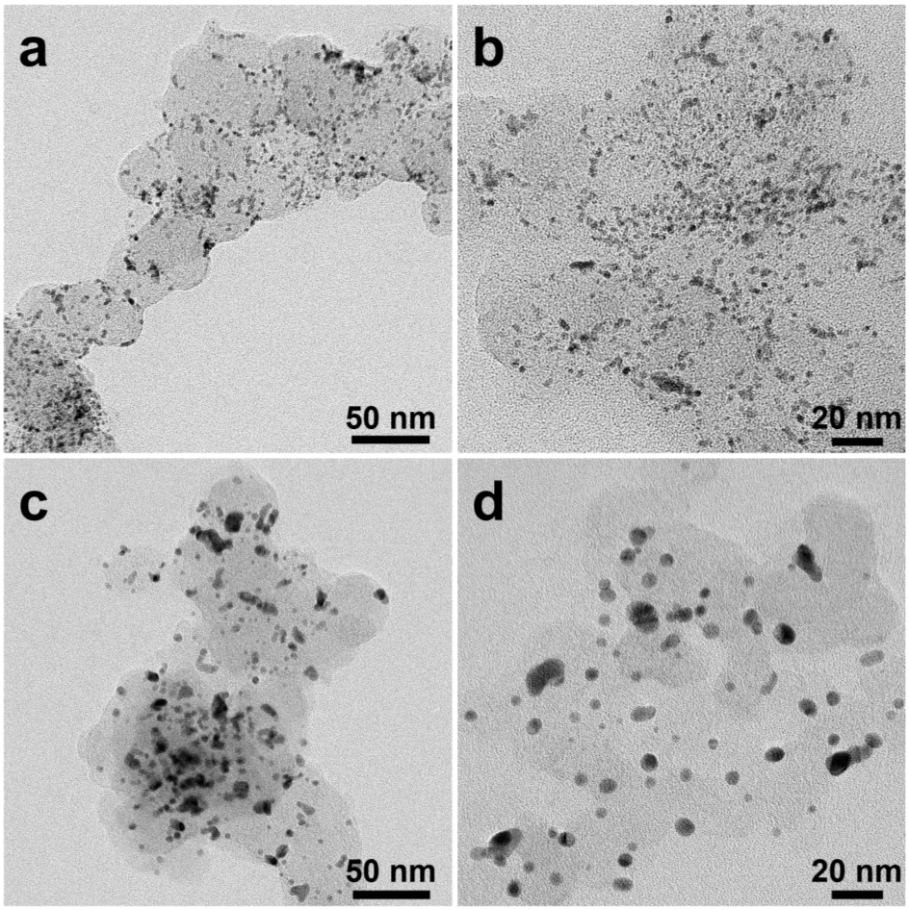

Figure S22. (a, b) TEM images of commercial Pt/C. (c, d) TEM images of commercial Pt/C after 30,000 cycles.

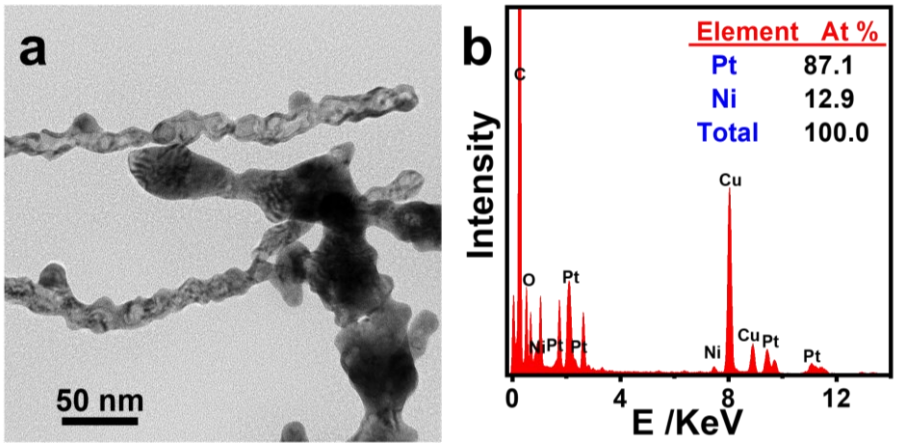

Figure S23. (a) TEM image and (b) TEM-EDS pattern of D-PtNi NWs/C after 30,000 cycles.

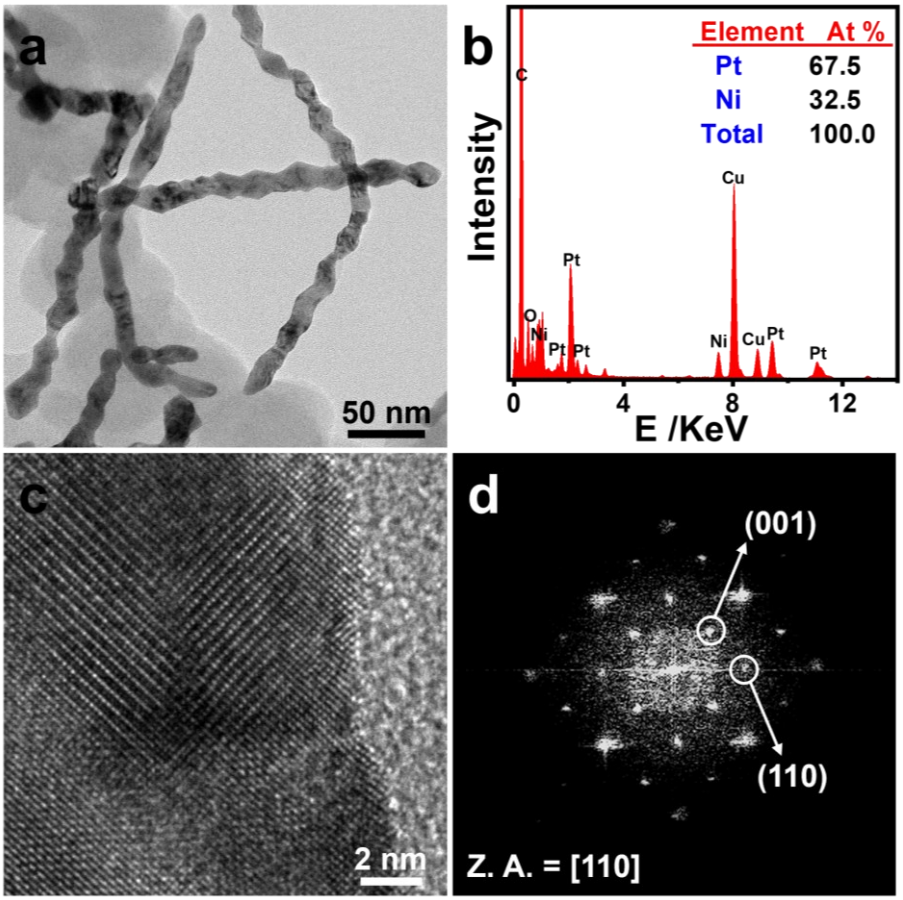

Figure S24. (a) TEM image, (b) TEM-EDS pattern, (c) HRTEM image and (d) corresponding FFT pattern of M-PtNi NWs/C after 30,000 cycles.

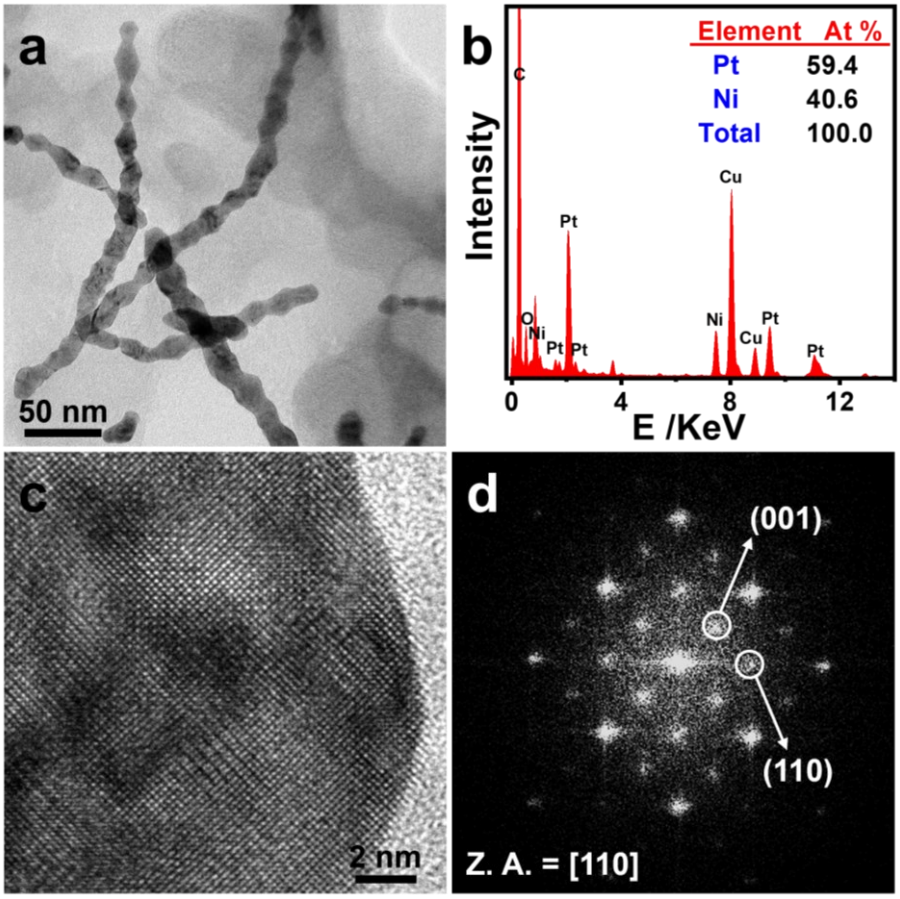

Figure S25. (a) TEM image, (b) TEM-EDS pattern, (c) HRTEM image and (d) corresponding FFT pattern of H-PtNi NWs/C after 30,000 cycles.

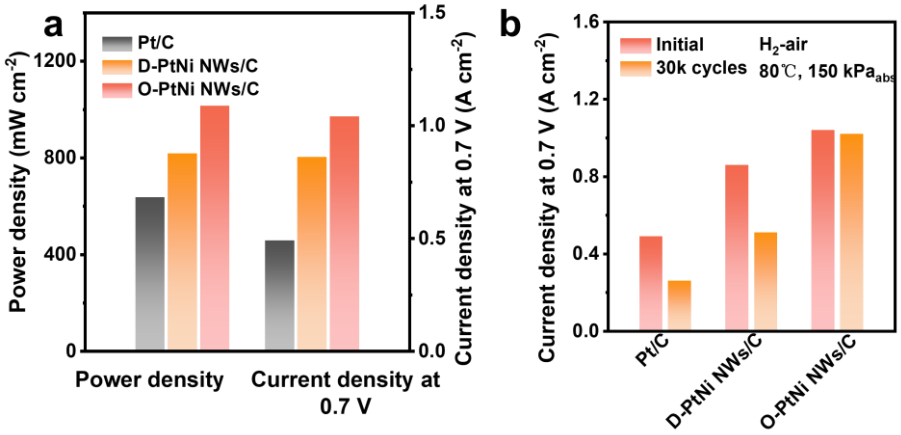

Figure S26. (a) Comparison of peak power density and current density at 0.7 V for different catalysts. (b) Changes in current density at 0.7 V of different catalysts before and after the AST.

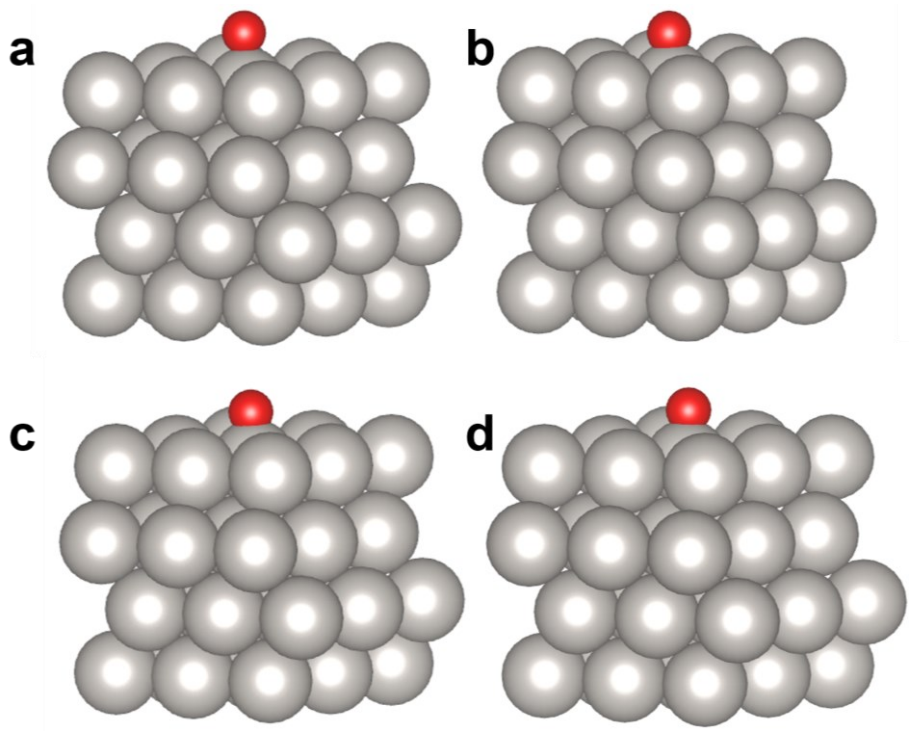

Figure S27. Adsorption configurations of O on the Pt(111) surface under (a) 0%, (b) 2%, (c) 5% and (d) 7% compressive strain. Gray and red spheres denote Pt and O atoms, respectively.

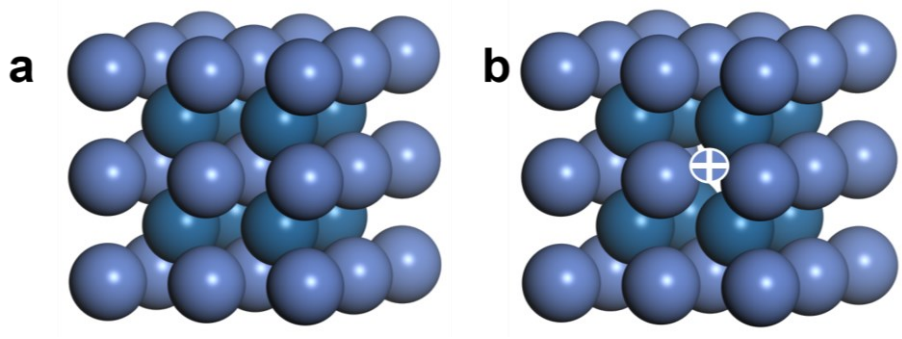

Figure S28. (a) Structural model of $L1_0$-PtNi and (b) $L1_0$-PtNi model containing a Ni vacancy. Blue and purple spheres represent Pt and Ni atoms, respectively.

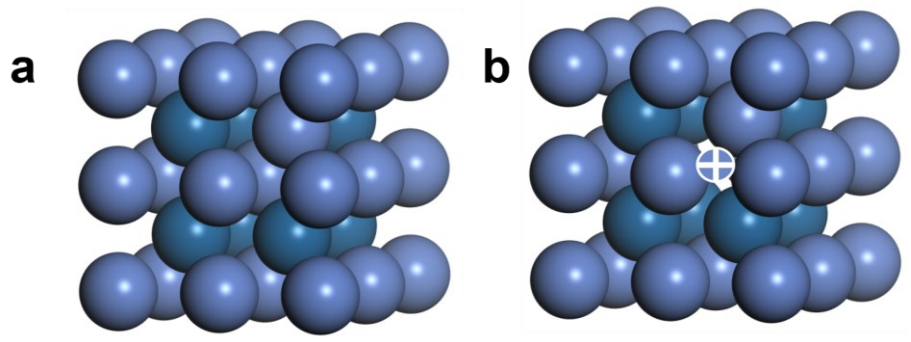

Figure S29.(a) Model of $L1_0$-PtNi in which one Pt atom adjacent to a Ni atom is substituted by Ni to emulate the local atomic environment of Ni in fcc-PtNi. (b) Corresponding structure shown in (a) with a Ni vacancy. Blue and purple spheres denote Pt and Ni atoms, respectively.

Table S1. Surface chemical states of Pt and Ni species in D-PtNi NWs/C, M-PtNi NWs/C and H-PtNi NWs/C determined from XPS analysis.

Sample	Pt^0/Pt^{2+}	Ni^0/Ni^{2+}
D-PtNi NWs/C	50.31/49.69	27.28/72.72
M-PtNi NWs/C	83.24/16.76	44.60/55.40
H-PtNi NWs/C	88.89/11.11	54.65/45.35

Table S2. Structural parameters of Pt foil, D-PtNi NWs/C, M-PtNi NWs/C and H-PtNi NWs/C extracted from the EXAFS fitting (S_0^2 = 0.854).

Sample	Path	CN	R (Å)	σ^2 (Å^2)	ΔE (eV)	R-factor
Pt-foil	Pt-Pt	12	2.77	0.004	7.86	0.0039
D-PtNi NWs/C	Pt-Pt	3.26	2.66	0.004	6.32	0.0035
	Pt-Ni	5.94	2.60	0.006		
M-PtNi NWs/C	Pt-Pt	3.67	2.68	0.008	6.81	0.0093
	Pt-Ni	6.41	2.60	0.003		
H-PtNi NWs/C	Pt-Pt	3.42	2.69	0.004	7.34	0.0023
	Pt-Ni	6.52	2.61	0.006		

Note: CN is the coordination number; R is interatomic distance; σ^2 is the Debye-Waller factor (a measure of thermal and static disorder in absorber-scatterer distances); R-factor is used to value the goodness of the fitting.

Table S3. Structural parameters of D-PtNi NWs/C, I-PtNi NWs/C-2 h, M-PtNi NWs/C, I-PtNi NWs/C-12 h and H-PtNi NWs/C obtained from XRD analysis.

Sample	2theta (°)	d (nm)	Compressive strain (%)
D-PtNi NWs/C	42.04079	0.21475	5.19
I-PtNi NWs/C-2 h	42.01223	0.21489	5.13
M-PtNi NWs/C	41.98965	0.21500	5.08
I-PtNi NWs/C-12 h	41.96707	0.21511	5.03
H-PtNi NWs/C	41.92439	0.21532	4.93

Structural parameters of PtNi nanowire catalysts with different degrees of ordering derived from X-ray diffraction (XRD) analysis. The 2theta values correspond to the (111) diffraction peaks, from which the interplanar spacing was calculated using Bragg's equation. The compressive strain was determined by comparing d (111) with that of pure Pt (0.2265 nm). A gradual decrease in 2theta and corresponding increase in d (111) indicate lattice relaxation as the ordering degree increases.